Electric Power Systems Research 96 (2013) 91–100

Contents lists available at SciVerse ScienceDirect

Electric Power Systems Research

journal homepage: www.elsevier.com/locate/epsr

Under voltage load shedding in power systems with wind turbine-driven doubly fed induction generators

Ardiaty Arief[a,*], ZhaoYang Dong[b], Muhammad Bachtiar Nappu[a], Marcus Gallagher[c]

[a] Department of Electrical Engineering, University of Hasanuddin, Makassar SULSEL 90213, Indonesia
[b] EA Centre of Excellence of Intelligent Electricity Networks, University of Newcastle, Callaghan, NSW, 2308, Australia
[c] School of Information Technology and Electrical Engineering, University of Queensland, St Lucia, Brisbane, QLD 4072, Australia

ARTICLE INFO

Article history:
Received 21 March 2012
Received in revised form 18 October 2012
Accepted 25 October 2012
Available online 8 December 2012

Keywords:
Doubly fed induction generator
Trajectory sensitivity
Under voltage load shedding
Voltage stability
Wind turbines

ABSTRACT

This paper presents the design and implementation of a new method of under voltage load shedding in a power system incorporating the use of wind generators to maintain voltage stability following a severe disturbance. This design considers the dynamic modeling of the load as well as the dynamic model of wind turbines. This work demonstrates a method to determine the minimum amount and the most appropriate location of load shedding. The proposed technique in this research involves an iterative algorithm based on trajectory sensitivity analysis to solve the load shedding problem. The load to be shed for each iteration is set at a small amount. Furthermore, the trajectory sensitivity factor (TSF) at all load buses and aggregated wind generator buses are calculated to provide information about the bus that has the prevalent influence in enhancing the system stability. The bus with the highest TSF is then selected as the location of the load shedding. This process is reiterated until the voltages at all buses are stable. Dynamic simulations are performed with the IEEE 14 bus Reliability Test System as a case study.

1. Introduction

The most popular wind generator technology installed in the power networks nowadays is the wind turbine-driven doubly fed induction generator (DFIG). The DFIG is a variable speed machine but can provide power with constant voltage and frequency as its rotor speed fluctuates. Furthermore, when a bidirectional converter is installed in the rotor, the range of rotor speed can be prolonged beyond the synchronous speed; hence, the electrical power is produced from both the stator and the rotor [1]. The DFIG has several advantages, such as a variable speed operation to obtain the maximum power extracted from the wind, adaptable power factor, better efficiency, ability to control the reactive power without capacitive support and less converter rating [2,3].

The high penetration of wind power generation in the network will affect the system's stability, especially the voltage stability; hence, the effect of the DFIG on system stability has become the subject of intense research during the past few years [4–10]. One issue that has not received much attention so far is load shedding in a power system with wind generators. Under voltage load shedding (UVLS) plays a vital part in power system control when the system is subjected to large disturbances. Research has validated that UVLS is an effectual counter-measure against voltage collapse. With the integration of large numbers of wind generators into the network, there is a requirement for the system operator to maintain the wind generators to keep supplying power to the system when the system voltage collapse occurs rather than being disconnected [11]. Nevertheless, because the DFIG stator is linked directly to the system and the limitation of excitation converter ratings, the DFIG can supply asynchronous power to the grid and be rather responsive to disruptions [12]. When the power system is subjected to a large disturbance, the DFIG transfers decreases power to the system. The inequity between the mechanical and electrical power in the generator speeds up the wind turbine; hence, its speed becomes faster [13]. As the speed is augmented, the DFIG then attracts more reactive power hence causing the system voltage to drop. After the fault is cleared, the DFIG is able to restore its normal operating condition only if the speed of the generator does not go over its critical speed [14]. Therefore, in a UVLS design this issue must be considered, so that the UVLS scheme can ensure that the DFIG can restore its normal operating condition and the system voltage can recover back to its stability limit.

The study in [15] proposes a UVLS design in a power system with distributed generations (DG), but this study only uses the static voltage analysis approach and does not consider the DG type. The drawback of such a technique is it cannot clarify the dynamic nature of the voltage collapse incidents. Additionally, with the widespread installation of wind generators and other DGs, the dynamic

* Corresponding author. Tel.: +62 812 41 693 693.
E-mail addresses: aarief@ft.unhas.ac.id, ardiaty@engineer.com (A. Arief), zydong@ieee.org (Z. Dong), bachtiar@ieee.org (M.B. Nappu), marcusg@itee.uq.edu.au (M. Gallagher).

0378-7796/$ – see front matter © 2012 Elsevier B.V. All rights reserved.
http://dx.doi.org/10.1016/j.epsr.2012.10.013

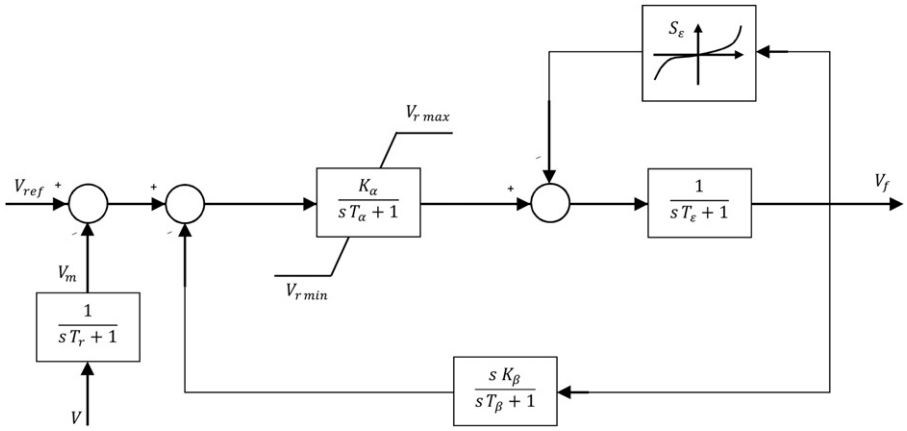

Fig. 1. Standard IEEE AVR type 1 excitation system model [24].

behavior of the system will change substantially after being perturbed because of the different technologies of the DGs and conventional generators [16].

In this paper, a novel analytical method is proposed to design a UVLS incorporating trajectory sensitivity analysis as a technique to determine the amount and location for load shedding and also observing the DFIG behavior after the system has been perturbed. The proposed method involves an iterative process that calculates the bus voltage trajectory sensitivities with respect to the load-shedding amount. At each step, the load shedding is set to a small amount. In addition, a new formulation, namely, the trajectory sensitivity factor (TSF) based on voltage trajectory sensitivities is employed to determine the load shedding location.

This paper is organized as follows. Section 2 provides an overview of the fundamental principles and current schemes of UVLS. Section 3 provides the details of a control system which is an automatic voltage and DFIG control system. Section 4 elaborates the proposed method for the trajectory sensitivity-based UVLS design. Section 5 gives the results and analysis, and Section 6 concludes the main findings of the research.

2. Power system under voltage load shedding

UVLS is an economical option to maintain voltage stability while waiting for the completion of new generation or transmission line projects [17]. Many utilities around the world have applied UVLS schemes. Imai [18] provided examples of existing UVLS applications in some utilities with their specific setting. The philosophy of UVLS is that whenever the system is disrupted, leading to voltage drop conditions below a certain pre-selected level for a certain predetermined time period, then selected loads should be removed [19]. It is expected that the system voltage will be restored to its normal limit by cutting off some loads. The objective of a UVLS is to reinstate the balance power within the system, to avert voltage collapse and to manage the voltage problems residing within a local area rather than permitting the problem to spread out to other areas [20]. The design of a load shedding should be "robust". UVLS must cover enough loads and must not be overly sensitive. Therefore, there are some considerations to ensure efficient load shedding as follows [19,21]:

- *Determination of amount of load to be shed*: Shedding an adequate amount of load is imperative in order to ensure UVLS can mitigate the menace of voltage instability. Shedding an insufficient amount of the necessary load will not be effective in arresting voltage collapse; on the other hand, shedding more load than required may lead to an over frequency circumstance.
- *Selection of location of load to be shed*: The study in [22] shows that shedding load in the correct location can arrest voltage instability. However, shedding the same amount of load in a different location gives a different result and may not be effective to improve the system stability.
- *Determination of timing and time steps of load shedding*: Load shedding is executed in steps in order to preclude the condition of over shedding. The minimum time delay before UVLS is triggered should be sufficient to prevent voltage collapse as well as to avoid unnecessary tripping during the transient time where load shedding is unnecessary.

Currently, there are two UVLS schemes being installed: decentralized (or distributed) UVLS, and centralized UVLS [19]. In both types, under voltage relays are set up at primary distribution substations which are near to major transmission substations to gauge the voltage at the transmission system. The decentralized system has better reliability than the centralized system because of its diversification. Failure of one element will not destructively intrude on the operation of other load shedding components. Load shedding in this scheme is concentrated to definite areas where the instability consequences are felt most sturdily. However, in a centralized scheme, under voltage appraising relays are sited at the most appropriate location in the system, not constrained to be close to a suitable load. The system voltages are observed at chosen strategic locations, which are usually the vital supply buses. In these crucial buses, the voltage level is securely controlled under the usual setting. In this structure, a verdict to execute load shedding is taken after significant low voltages transpire throughout the system by means of communications between primary localities.

3. Automatic voltage regulator and DFIG control system

3.1. Automatic voltage regulator

Modern generators are prepared with an automatic voltage regulator (AVR). An AVR outlines the primary voltage regulation of the generator and its function is to sustain the constant terminal voltage and to monitor the reactive power output [23]. An AVR also improves the generator stability margin. In this paper, the standard IEEE AVR type 1 excitation system model is employed as in Fig. 1 [24].

3.2. DFIG control system

A typical configuration of a DFIG wind turbine technology is shown schematically in Fig. 2. The stator and rotor flux dynamic

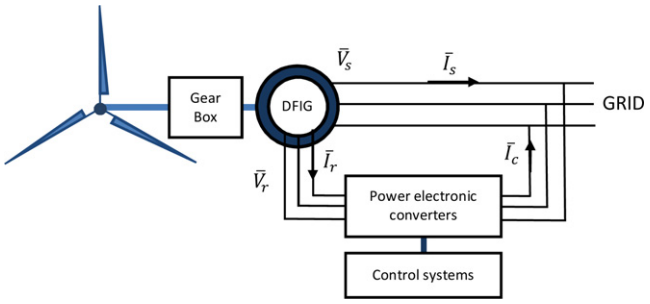

Fig. 2. DFIG wind turbine technology configuration.

are fast compared to the grid dynamic and the control systems of the converter decouple the generator from the grid; hence, the steady-state electrical equations of the DFIG are considered, so that [25]:

$$\upsilon_{ds} = -rsi_{ds} + [(x_s + x_m)i_{qs} + x_m i_{qr}] \quad (1)$$

$$\upsilon_{qs} = -r_s i_{qs} - [(x_s + x_m)i_{ds} + x_m i_{dr}] \quad (2)$$

$$\upsilon_{dr} = -r_R i_{dr} + (1 - \omega_m)[(x_R + x_m)i_{qr} + x_m i_{qs}] \quad (3)$$

$$\upsilon_{qr} = -r_R i_{dr} + (1 - \omega_m)[(x_R + x_m)i_{dr} + x_m i_{ds}] \quad (4)$$

Then, the active and reactive power delivered to the grid become:

$$P = \upsilon_{ds} i_{ds} + \upsilon_{qs} i_{qs} + \upsilon_{dc} i_{dc} + \upsilon_{qc} i_{qc} \quad (5)$$

$$Q = \upsilon_{qs} i_{qs} - \upsilon_{ds} i_{ds} + \upsilon_{qc} i_{qc} - \upsilon_{dc} i_{dc} \quad (6)$$

Since the converter dynamics are fast in comparison with the electromechanical transients, the converter is simplified and modeled as an ideal current source where i_{qr} and i_{dr} are state variables. i_{qr} is employed for the rotor speed control, while i_{dr} is used for voltage control. The schemes of the DFIG rotor speed control and voltage control are given in Figs. 3 and 4, respectively.

Differential equations for the converter currents can be written as:

$$i_{qr} = \left[-\frac{x_s + x_m}{x_m V} \frac{P^*_\omega(\omega_m)}{\omega_m} - i_{qr} \right] \frac{1}{T_\in} \quad (7)$$

$$i_{dr} = K_V(V - V_{ref}) - \frac{V}{x_m} - i_{dr} \quad (8)$$

$P^*_\omega(\omega_m)$ is the power-speed characteristic that optimizes the wind energy capture and is calculated using the rotor speed value.

4. Trajectory sensitivities enhanced UVLS scheme

4.1. Trajectory sensitivity analysis

Trajectory sensitivity analysis is a technique based on linearizing a system surrounding a certain trajectory and employs time domain simulations [26]. This technique computes the sensitivity of the dynamics relating to the constraints [27]. Trajectory sensitivity provides a method of enumerating changes in the system variables in connection with the quick changes of system parameters and initial conditions [28]. The basic methodology of trajectory sensitivity computation of hybrid systems is illustrated in [28], and is discussed as follows.

The systematic representation of a power system which is applicable to voltage stability study is provided by the following differential-algebraic equation (DAE):

$$\dot{x} = f(x, y; \quad \alpha) \quad (9)$$

$$0 = g(x, y; \quad \alpha) \quad (10)$$

where x is the vector of the dynamic state variables; y is the vector of the algebraic state variables such as load bus voltage magnitudes and angles; and α represents system parameters, such as power at the bus.

The trajectories of (9) and (10) illustrate the performance of the dynamic variables x and algebraic variables y, where the flows of x and y can be defined, as:

$$x(t) = \varphi_x(x_0, t, \alpha) \quad (11)$$

$$y(t) = \varphi_y(y_0, t, \alpha) \quad (12)$$

Sensitivities of the flows φ_x and φ_y to the initial conditions and parameter variations can be acquired by forming the Taylor series

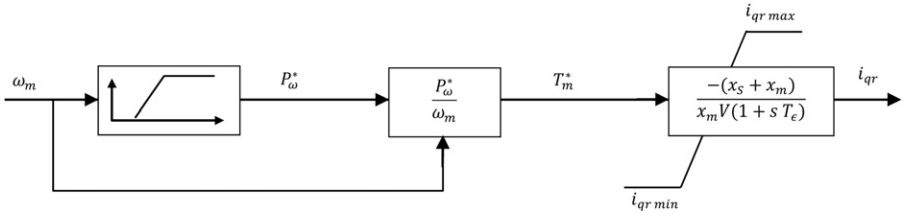

Fig. 3. DFIG rotor speed control [25].

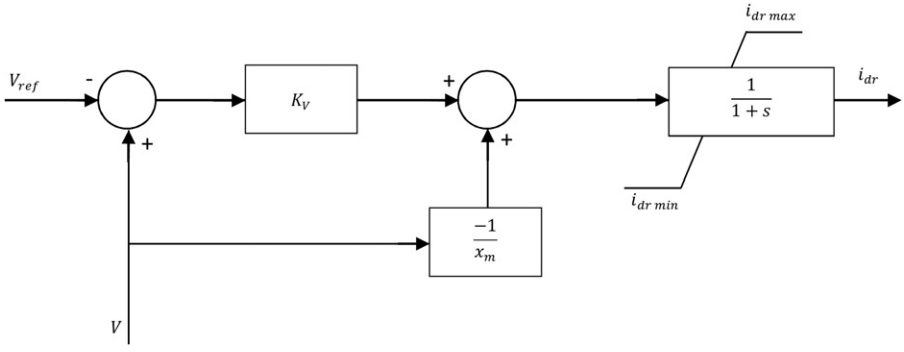

Fig. 4. DFIG voltage control [25].

expansions of the above equations, hence:

$$\Delta x(t) = \Delta\varphi_x(x_0, t, \alpha) = \frac{\partial\varphi_x(x, t, \alpha)}{\partial\alpha}\Delta\alpha = \frac{\partial x(t)}{\partial\alpha}\Delta\alpha \cong x_\alpha(t)\Delta\alpha \tag{13}$$

$$\Delta y(t) = \Delta\varphi_y(y_0, t, \alpha) = \frac{\partial\varphi_y(y_0, t, \alpha)}{\partial\alpha}\Delta\alpha = \frac{\partial y(t)}{\partial\alpha}\Delta\alpha \cong \sim y_\alpha(t)\Delta\alpha \tag{14}$$

An approximation-based numerical method is used to compute the sensitivities x_α and y_α, consequently:

$$x_\alpha = \frac{\partial x}{\partial\alpha} = \frac{\Delta x}{\Delta\alpha} \approx \frac{\varphi_x(x_0, t, \alpha + \Delta\alpha) - \varphi_x(x_0, t, \alpha)}{\Delta\alpha} \tag{15}$$

$$y_\alpha = \frac{\partial y}{\partial\alpha} = \frac{\Delta y}{\Delta\alpha} \approx \frac{\varphi_y(y_0, t, \alpha + \Delta\alpha) - \varphi_y(y_0, t, \alpha)}{\Delta\alpha} \tag{16}$$

The trajectory sensitivities from (14) and (16) are revised to meet the purpose of this study. The bus voltage magnitude and load shedding amount are both parameters represented by y and α correspondingly; hence, the sensitivities of the bus voltage variation after load shedding at any specified bus are computed and can be defined as:

$$\Delta V(t) = \Delta\varphi_V(V_0, t, P) = \frac{\partial\varphi_V(V_0, t, P)}{\partial P}\Delta P = \frac{\partial V(t)}{\partial P}\Delta P \cong V_P(t)\Delta P \tag{17}$$

$$\varphi V_P = \frac{\partial V}{\partial P} = \frac{\Delta V}{\Delta P} \approx \frac{\varphi_V(V_0, t, P + \Delta P) - \varphi_V(V_0, t, P)}{\Delta P} \tag{18}$$

4.2. Trajectory sensitivity factor

In addition, the trajectory sensitivities are performed to find the load shedding location. A trajectory sensitivity factor is formulated to assess the contribution of bus j after load shedding to the system voltage stability. The sensitivities calculated are $[\partial V_i/\partial P_j]$, which inform the rate of change in voltage magnitude at bus i with respect to the load shedding amount variation at bus j. The TSF at bus j is computed by shedding the active power at bus j by a small value, then assessing its impact on voltage magnitudes at all the critical buses along the time domain. The TSF proposed in this work is defined as:

$$TSF_j = TSF_j^{load} + TSF_j^{wind} \tag{19}$$

$$TSF_j^{load} = \sum_{i=1}^{n_k}\left[\sum_{t=0}^{t_s}\left[\frac{\partial V_i^{load}}{\partial P_j}\right]_{t=t_k}\right] \tag{20}$$

$$TSF_j^{wind} = \sum_{i=1}^{n_{wind}}\left[\sum_{t=0}^{t_s}\left[\frac{\partial V_i^{wind}}{\partial P_j}\right]_{t=t_k}\right] \tag{21}$$

$$\partial P_j = \Delta P_j = P_{shed_j}$$

where P_{shed_j}, load shedding amount at bus j; n_k, number of critical buses; n_{wind}, number of aggregated DFIG buses; t_k, time instant; t_s, number of time instants.

There are two components computed here: TSF_j^{load} and TSF_j^{wind}. TSF_j^{load} evaluates the voltage trajectory sensitivities at critical load buses with respect to the load shedding at bus j, whereas TSF_j^{wind} assesses the voltage sensitivities at the wind turbine buses with respect to the load shedding at bus j. The bus with the highest TSF has the largest effect on the voltage stability improvement of the critical buses and hence will be selected as a candidate bus for the location of the UVLS. The flowchart of the proposed trajectory sensitivity-based UVLS is shown in Fig. 5 and can be explained as follows:

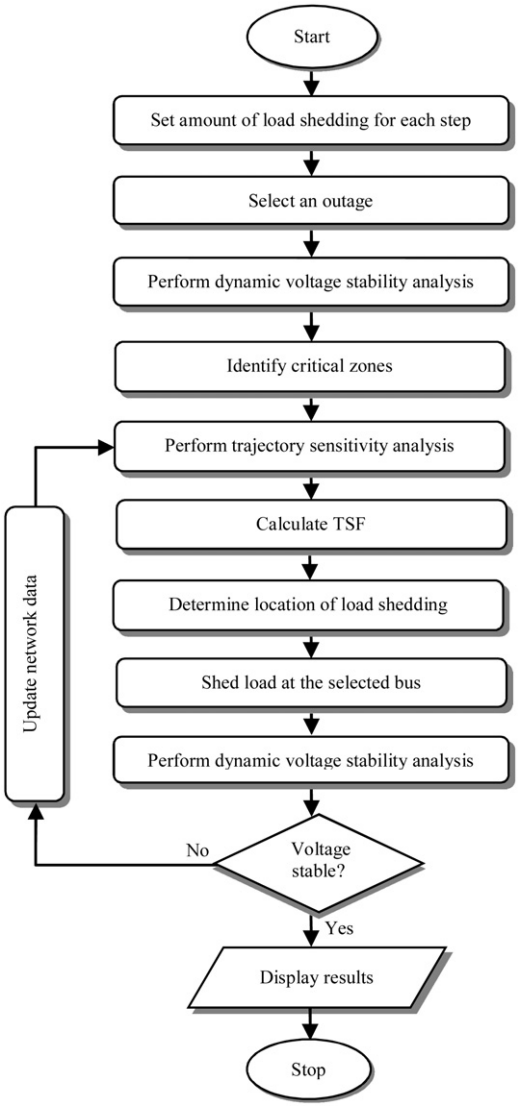

Fig. 5. Flowchart of the trajectory sensitivity-based UVLS design.

Step 1 Set the load shedding amount. In this work, the load shedding amount is set at 5 MW for each iteration.
Step 2 Select an outage.
Step 3 Perform dynamic voltage stability analysis to observe the voltage behavior for all buses.
Step 4 Identify critical zones. This is a zone where buses have a similar pattern of voltage drop.
Step 5 Perform trajectory sensitivity analysis to evaluate the bus voltage trajectory sensitivities.
Step 6 Calculate TSF to assess the contribution of each load bus on improving the voltage stability of the buses at the critical zones. The bus with the highest TSF has the most influence on improving the system voltage magnitude. The location of load shedding is determined based on the highest TSF value.
Step 7 Apply load shedding in the selected bus.
Step 8 Perform dynamic voltage stability analysis to evaluate the system performance after load shedding.

Step 9 If the system is still unstable, then the network data is updated; go to Step 5. This process will be reiterated until the voltage stability constraint is satisfied.

Step 10 If the voltage stability requirement has been fulfilled, then write the results and stop the process.

5. Simulation results

5.1. Without DFIG connected to the system

The proposed method is implemented at the IEEE 14 bus Reliability Test System (Fig. 6). The system is assumed to be working on a stressed condition. The system load for this study is 511.36 MW, consisting of 50% static load and 50% dynamic motor load. The detail of the load modeling can be seen in [29]. Prior to designing the UVLS scheme, contingency analysis is performed to choose the critical outage. Based on this analysis, the outage between bus 6 and bus 13 is chosen in this study. For the dynamic simulation, a fault is applied between bus 6 and bus 13, and then the fault is cleared by removing the transmission line between bus 6 and bus 13. Firstly, we evaluate the UVLS design without any wind generator. Fig. 7(a) shows the voltage drop after disturbance. There are five critical buses at which the voltage collapses below the stability limit (0.9 pu). They are buses 9, 10, 12, 13 and 14 as shown in Fig. 7(b).

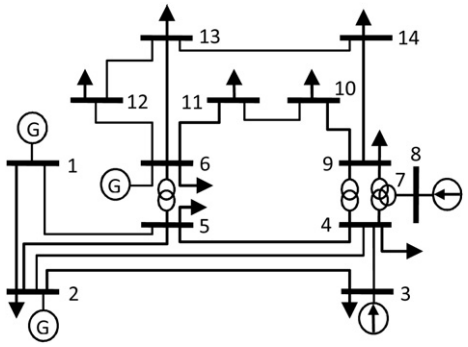

Fig. 6. The test system—IEEE 14 Bus Reliability Test System.

For this simulation, the load-shedding amount for each iteration is set at approximately 1% of the total system load. In this case, we round the amount to 5 MW for each step. The trajectory sensitivity analysis is performed to assess the effect of load shedding of 5 MW at each bus in the critical zone. Fig. 8(a) and (b) illustrates the voltage trajectory sensitivities of critical buses for the first iteration if load shedding is commenced at bus 14 and bus 6, respectively. From both of these figures, it can be concluded that the voltage trajectory sensitivities if load shedding occurs at bus 14 are better than the

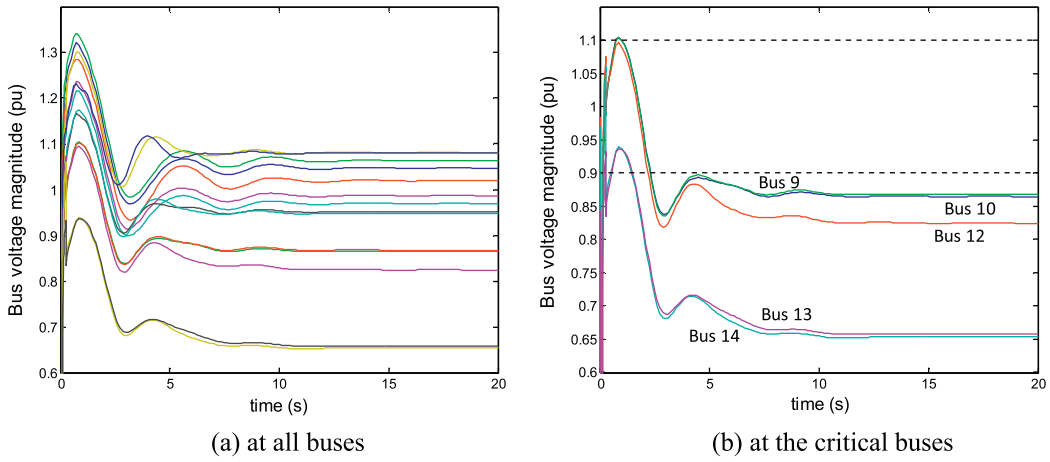

Fig. 7. Voltage drop after outage between bus 6 and bus 13 without DFIG.

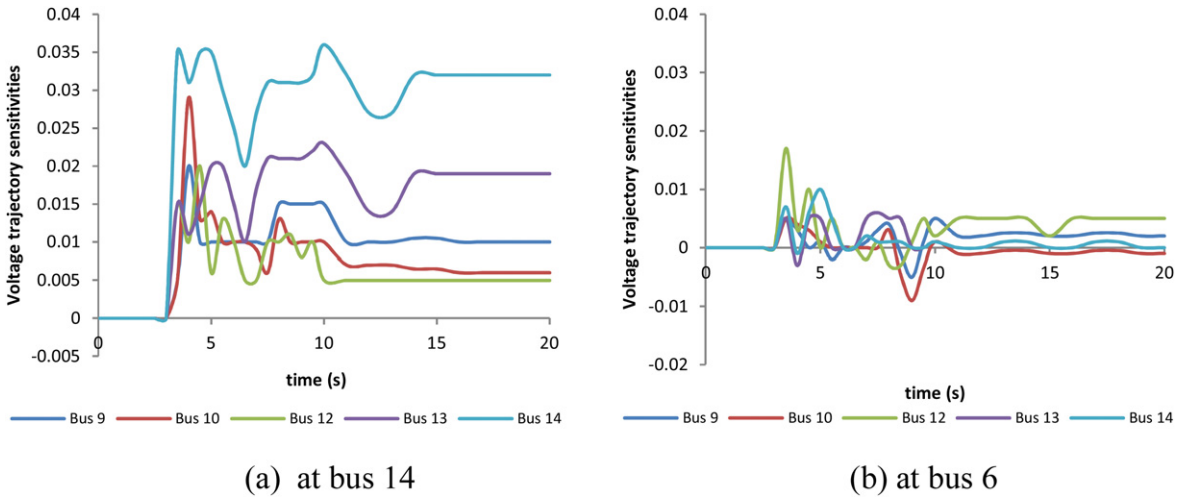

Fig. 8. Bus voltage trajectory sensitivities of critical buses if load shedding is 5 MW. (For interpretation of the references to color in text, the reader is referred to the web version of this article.)

Table 1
TSF calculation for case without DFIG.

$$\sum_{t=0}^{t_s}\left[\frac{\partial V_i^{load}}{\partial P_j}\right]_{t=t_k}$$

Bus j / Bus i	14	6
9	0.271	0.037
10	0.223	−0.008
12	0.188	0.083
13	0.432	0.038
14	0.74	0.037
TSF_j^{load}	1.854	0.187

Table 2
TSF values for case without DFIG.

Iteration / Bus number	TSF value I	II	III	IV	V	VI
2	0.205	0.134	0.110	0.098	0.074	0.026
3	0.211	0.167	0.149	0.106	0.079	0.034
4	0.398	0.302	0.257	0.211	0.086	0.057
5	0.342	0.264	0.216	0.174	0.123	0.089
6	0.187	0.112	0.098	0.077	0.056	0.034
9	0.978	0.849	0.798	0.731	0.674	0.324
10	1.125	1.046	0.987	0.923	0.879	0.585
11	1.302	1.213	1.168	1.092	1.021	0.793
12	1.324	1.265	1.205	1.158	1.115	0.967
13	1.743	1.419	1.367	1.257	1.187	1.076
14	1.854	1.578	1.319	1.296	1.159	1.025

sensitivities at bus 6. Furthermore, TSF is calculated to provide a distinct indication for load shedding location. Here, we only compute the TSF_j^{load} since there are no wind generators yet. In computing the TSF_j^{load} value, we use time interval 0.5 s for the period 0–20 s. Table 1 illustrates the TSF_j^{load} calculation for load shedding at bus 14 and bus 6.

Fig. 9 depicts the TSF value for each load bus at the first iteration. As indicated in the red bar, bus 14 has the highest TSF (1.854). Load shedding of 5 MW is simulated at bus 14 and the system voltage magnitude is re-evaluated. At this stage, the system is still unstable; hence, trajectory sensitivities are performed again to calculate the TSF. For this simulation, this process is repeated six times until the system voltages are stable (above 0.9 pu). The results of the TSF calculation for each iteration and load shedding location based on the highest TSF are presented in Tables 2 and 3, respectively. Hence, the load shedding locations are bus 14 and bus 13 with a load shedding amount at each bus of 15 MW. The results of the

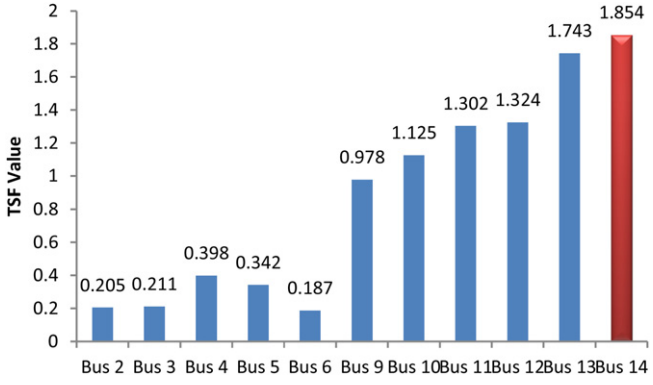

Fig. 9. TSF values at first iteration without DFIG.

Table 3
Load shedding locations for case without DFIG.

Iteration	Load shedding design	
	Location	Amount (MW)
I	Bus 14	5
II	Bus 14	5
III	Bus 13	5
IV	Bus 14	5
V	Bus 13	5
VI	Bus 13	5

Table 4
DFIG parameters.

Power rating	2 MVA
Voltage rating	13.8 kV
Frequency rating	60 Hz
Stator resistance (R_s)	0.01 pu
Stator reactance (X_s)	0.10 pu
Rotor resistance (R_r)	0.01 pu
Rotor reactance (X_r)	0.08 pu
Magnetization reactance (X_m)	3.00 pu
Inertia Constants	3 kWs/kVA

voltage improvement after load shedding of 30 MW at bus 14 and bus 13 can be seen in Fig. 10. It clearly proves that the voltages at all buses improve significantly and that the system stability is recovered.

5.2. With DFIG connected to bus 14

5.2.1. Determination of amount and location of load shedding

To evaluate the UVLS scheme with wind generators, we postulate that aggregated DFIGs are connected to bus 14 with a total accumulative power of 10 MW. The details of the wind generator parameters are shown in Table 4.

Fig. 11(a) portrays the voltage behavior at all buses following a disturbance between bus 6 and bus 13. Specifically, Fig. 11(b) illustrates the voltage drop at the critical buses, of which there are only three (buses 12, 13 and 14).

In order to assess the effect of load shedding on the critical load and DFIG buses, the trajectory sensitivity analysis is carried out. Fig. 12(a) and (b) shows the voltage trajectory sensitivities of critical buses for the first iteration if load shedding is undertaken at bus 14 and bus 13, correspondingly. It is clearly proven that the sensitivities if load shedding occurs in bus 13 are superior than if

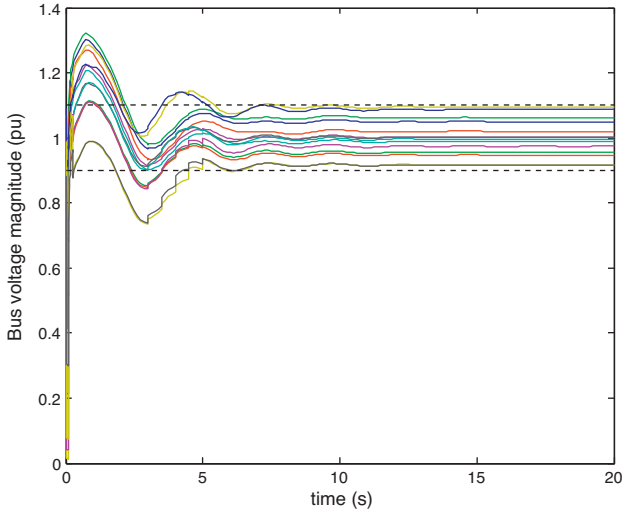

Fig. 10. Voltage profile improvement after load shedding without DFIG.

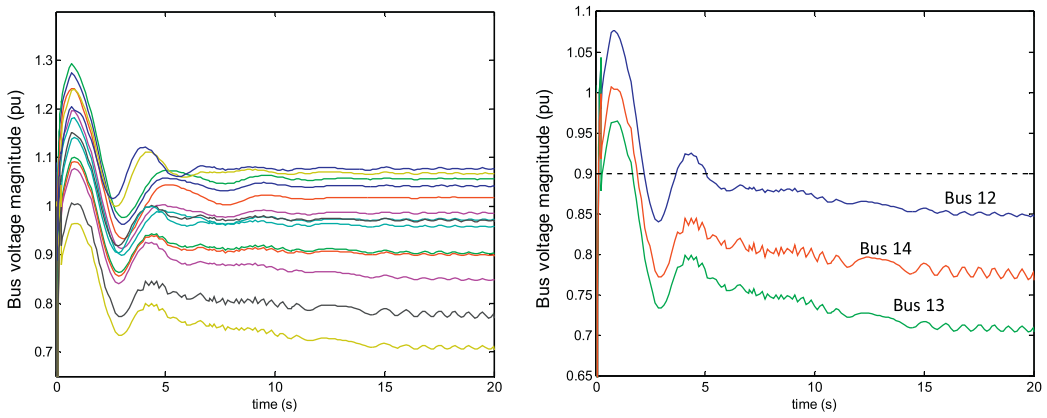

Fig. 11. Voltage drop after outage between bus 6 and bus 13 considering DFIG.

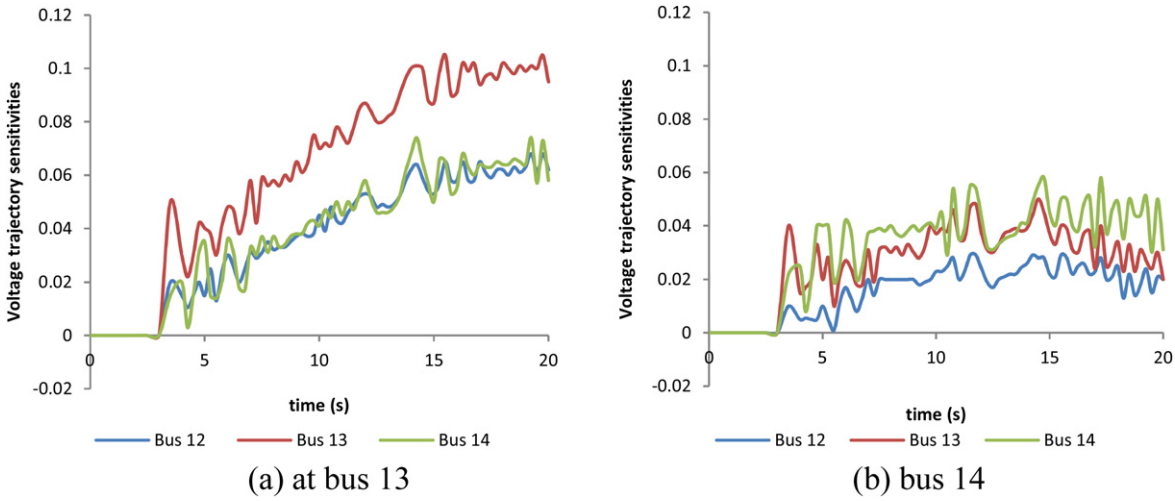

Fig. 12. Bus voltage trajectory sensitivities of critical buses if load shedding is 5 MW.

the load shedding occurs at bus 14. In addition, Fig. 13 presents the trajectory sensitivities of the aggregated DFIG voltage if load shedding occurs at buses 14, 13 and 3. It also shows that by load shedding in bus 13, the voltage sensitivities of the DFIG bus are greater than the sensitivities if load shedding occurs at bus 14 or 3. Nevertheless, in order to reach a better quantitative conclusion, the TSF is calculated, consisting of two components: the TSF_j^{load} and the TSF_j^{wind}. Similar to the computation without DFIG, the time interval used is also 0.5 s for the period 0–20 s. The TSF_j calculation for load shedding at buses 14, 13 and 3 is displayed in Table 5.

Fig. 14 conveys the results of the TSF calculation at all load buses. Interestingly, bus 14 no longer has the highest TSF. When the aggregated DFIGs are connected to bus 14, bus 13 now has the largest TSF. Therefore, this bus has the biggest influence on improving the system stability. For this condition, the sensitivity analysis procedure is iterated three times, and the results of this process are expressed in Table 6. After load shedding with a total amount of 15 MW (10 MW

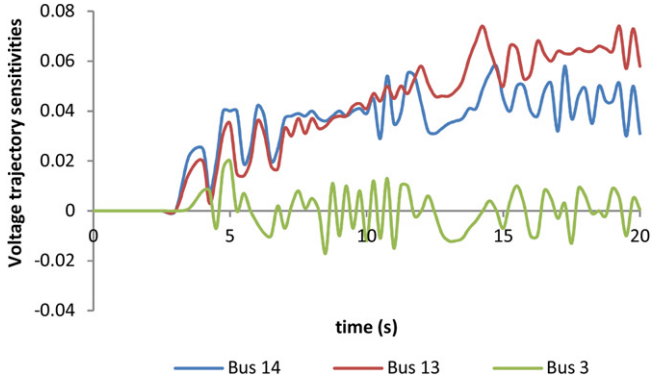

Fig. 13. DFIG voltage trajectory sensitivities with load shedding of 5 MW applied at buses 14, 13 and 3.

Table 5
TSF calculation for case considering DFIG.

Bus j	TSF_j^{load}	TSF_j^{wind}	TSF_j
3	0.0815	0.0365	0.118
13	2.054	0.812	2.866
14	0.851	0.658	1.509

Table 6
Load shedding locations for case considering DFIG.

Iteration	Load shedding design	
	Location	Amount (MW)
I	Bus 13	5
II	Bus 13	5
III	Bus 14	5

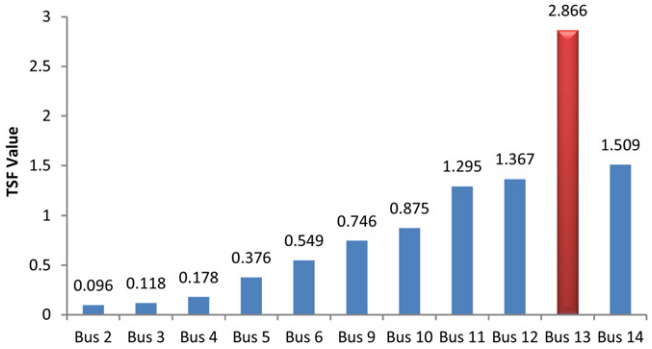

Fig. 14. TSF values at first iteration with DFIG.

at bus 13 and 5 MW at bus 14), the system voltage recovers to its stable condition with the result portrayed in Fig. 15. Table 7 summarizes the comparison of the UVLS design with and without the DFIG connected to the system. It is obvious that, with the integration of wind generators to the system, the UVLS scheme changes and reduces the amount of load to be disengaged from the system. The integration of DG brings positive effects on the voltage profile by providing additional system generation capacity including during outage.

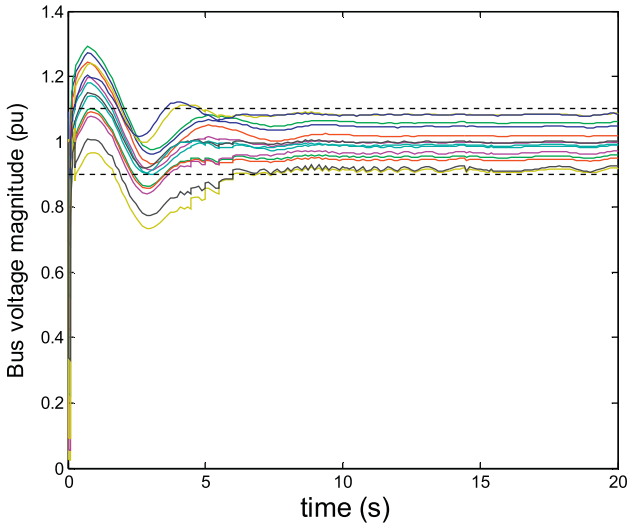

Fig. 15. Voltage profile improvement after load shedding with DFIG.

5.2.2. Analysis of DFIG behavior

Fig. 16(a–c) demonstrates the DFIG voltage behavior following outage between bus 6 and bus 13 before and after load shedding. Fig. 16(a) clearly shows that the DFIG voltage decreases to approximately 0.76 pu at $t = 20$ s. In addition, as mentioned in the

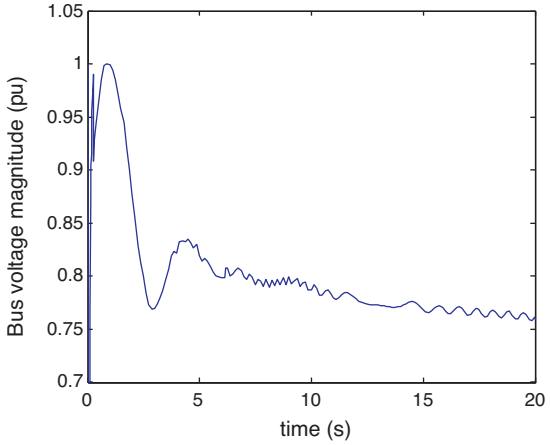

(a) voltage drop without load shedding

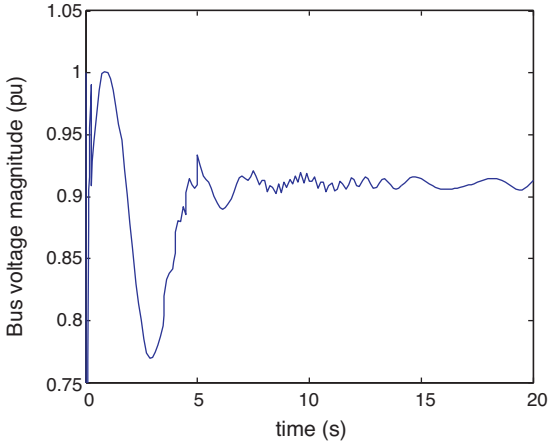

(b) after load shedding at bus 13 and bus 14

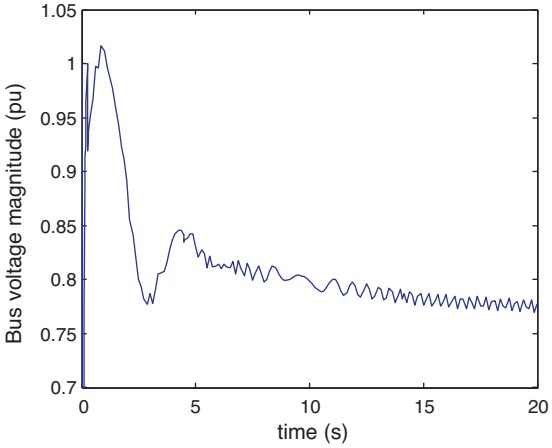

(c) after load shedding at bus 3

Fig. 16. Voltage behavior at DFIG bus.

Table 7
Comparison load shedding scheme with and without DFIG.

	Load shedding design		
	Location	Amount (MW)	Total (MW)
Without DFIG	Bus 14 Bus 13	15 15	30
With DFIG	Bus 13 Bus 14	10 5	15

introduction, because of this disturbance, the DFIG then supplies asynchornous power to the grid as a result of the excitation converter limitation and its stator that is linked directly to the grid. After load shedding at bus 13 and bus 14 (Fig. 16(b)), this asynchronous power still exists even though the DFIG voltage can recover back to its stable condition above 0.9 pu. However, this asynchronous power issue is outside the scope of this work since this work only focuses on determining the amount and location of load shedding to ensure the DFIG voltage can improve. Therefore, another interesting direction to take in further research would be to investigate UVLS design in power systems with DFIG to improve its voltage stability after a disturbance as well as reducing the asynchronous power generated after a disturbance.

Fig. 16(c) shows the voltage behavior at the DFIG bus after shedding a load of 15 MW at bus 3. From Table 5, bus 3 has low TSF (0.118) which means it has low impact on improving voltage stability. It shows that load shedding in this bus has no significant impact on improving DFIG voltage stability after being disturbed. The DFIG cannot restore its normal operating condition. Therefore, it is not recommended to shed load at a bus with low TSF.

6. Conclusion

This paper proposes a dynamic analysis-based design of UVLS for stabilizing the system following disturbance and ensuring the system's secure limits are satisfied. The design is based on a trajectory sensitivities technique that calculates the sensitivity of the dynamics relating to the constraints and provides a method of enumerating changes in the system variables in connection with the quick changes of system parameters and initial conditions. In this paper, trajectory sensitivities are employed to determine the minimum amount of the load shedding and to verify the location of the load shedding. The trajectory sensitivity factor provides useful information to find the best location for load shedding. The bus with the highest TSF has the largest effect on enhancing the voltage stability of the critical buses, and hence will be selected as a candidate bus for the location of the UVLS.

This work simulates the system behavior after being perturbed with and without the DFIG. From the simulations, it is seen that the installation of the DFIG can help the demand side management in critical situations by reducing the amount of load to be disconnected from the system. Before installation of the DFIG, the amount of load shedding is 30 MW; whereas, when the DFIG is connected with a total aggregated power of 10 MW, the load shedding amount decreases to 15 MW.

The proposed method provides significant voltage improvement and by using the proposed method, various power system failures after the system has been perturbed can be prevented, including in a power system with wind generators. This method can be applied robustly with or without wind generators and can be applied considering other types of DG as long as the DG unit is modeled accurately.

One problem with the integration of the DFIG is the asynchronous power generated following disturbance. Further research can be undertaken to analyze this issue and investigate how to improve UVLS performance by reducing this asynchronous power.

References

[1] R. Pena, J.C. Clare, G.M. Asher, A doubly fed induction generator using back-to-back PWM converters supplying an isolated load from a variable speed wind turbine, IEE Proceedings: Electric Power Applications 143 (1996) 380–387.
[2] N. Heng, S. Yipeng, Z. Peng, H. Yikang, Improved direct power control of a wind turbine driven doubly fed induction generator during transient grid voltage unbalance, IEEE Transactions on Energy Conversion 26 (2011) 976–986.
[3] E. Vittal, M. O'Malley, A. Keane, A steady-state voltage stability analysis of power systems with high penetrations of wind, IEEE Transactions on Power Systems 25 (2010) 433–442.
[4] V. Akhmatov, P.B. Eriksen, A large wind power system in almost island operation: a Danish case study, IEEE Transactions on Power Systems 22 (2007) 937–943.
[5] M.H. Ali, W. Bin, Comparison of stabilization methods for fixed-speed wind generator systems, IEEE Transactions on Power Delivery 25 (2010) 323–331.
[6] C. Chompooinwai, C. Yingvivatanapong, K. Methaprayoon, L. Wei-Jen, Reactive compensation techniques to improve the ride-through capability of wind turbine during disturbance, IEEE Transactions on Industry Applications 41 (2005) 666–672.
[7] M.J. Hossain, H.R. Pota, M.A. Mahmud, R.A. Ramos, Investigation of the impacts of large-scale wind power penetration on the angle and voltage stability of power systems, IEEE Systems Journal (2011) 1.
[8] H.T. Le, S. Santoso, T.Q. Nguyen, Augmenting wind power penetration and grid voltage stability limits using ESS: application design, sizing, and a case study, IEEE Transactions on Power Systems (2011) 1.
[9] U. Nayeem Rahmat, T. Torbjrn, Variable speed wind turbines for power system stability enhancement, IEEE Transactions on Energy Conversion 22 (2007) 52–60.
[10] E. Vittal, M. O'Malley, A. Keane, Rotor angle stability with high penetrations of wind generation, IEEE Transactions on Power Systems (2011) 1.
[11] W. Yi, X. Lie, Coordinated control of DFIG and FSIG-based wind farms under unbalanced grid conditions, IEEE Transactions on Power Delivery 25 (2010) 367–377.
[12] Z. Peng, H. Yikang, S. Dan, Improved direct power control of a DFIG-based wind turbine during network unbalance, IEEE Transactions on Power Electronics 24 (2009) 2465–2474.
[13] A. Arulampalam, M. Barnes, N. Jenkins, J.B. Ekanayake, Power quality and stability improvement of a wind farm using STATCOM supported with hybrid battery energy storage, IEE Proceedings Generation, Transmission and Distribution 153 (2006) 701–710.
[14] S.K. Salman, A.L.J. Teo, Windmill modelling consideration and factors influencing the stability of a grid-connected wind power-based embedded generator, IEEE Transaction on Power Systems 18 (2003) 793–802.
[15] X. Ding, A.A. Girgis, Optimal load shedding strategy in power systems with distributed generation, in: IEEE Power Engineering Society Winter Meeting, vol. 2, Columbus, OH, January 28–31, 2001, pp. 788–793.
[16] I. Erlich, J. Kretschmann, J. Fortmann, S. Mueller-Engelhardt, H. Wrede, Modeling of wind turbines based on doubly-fed induction generators for power system stability studies, IEEE Transactions on Power Systems 22 (2007) 909–919.
[17] Undervoltage Load Shedding Task Force (UVLSTF) Technical Studies Subcommittee, Undervoltage Load Shedding Guidelines, Western Systems Coordinating Council, July 1999.
[18] S. Imai, Undervoltage load shedding improving security as reasonable measure for extreme contingencies, in: IEEE Power Engineering Society General Meeting, vol. 2, San Francisco, CA, 12–16 June, 2005, pp. 1754–1759.
[19] M. Begovic, D. Fulton, M.R. Gonzalez, J. Goossens, E.A. Guro, R.W. Haas, C.F. Henville, G. Manchur, G.L. Michel, R.C. Pastore, J. Postforoosh, G.L. Schmitt, J.B. Williams, K. Zimmerman, A.A. Burzese, Summary of system protection and voltage stability, IEEE Transactions on Power Delivery 10 (1995) 631–638.
[20] C.J. Mozina, Undervoltage load shedding, in: 60th Annual Conference for Protective Relay Engineers, Texas, USA, 27–29 March, 2007, pp. 16–34.
[21] S.S. Ladhani, W. Rosehart, Under voltage load shedding for voltage stability overview of concepts and principles, in: IEEE Power Engineering Society General Meeting, vol. 2, Denver, CO, 6–10 June, 2004, pp. 1597–1602.
[22] C.M. Affonso, L.C.P. da Silva, F.G.M. Lima, S. Soares, MW and MVar management on supply and demand side for meeting voltage stability margin criteria, IEEE Transactions on Power Systems 19 (2004) 1538–1545.
[23] J.B.X. Devotta, A dynamic model of the synchronous generator excitation control system, IEEE Transactions on Industrial Electronics 34 (1987) 429–432.
[24] IEEE Committee Report, Excitation system models for power system stability studies, IEEE Transactions on Power Apparatus and Systems PAS-100 (1981) 494–509.
[25] F. Milano, Power System Analysis Toolbox, 2005.

[26] K.N. Shubhanga, A.M. Kulkarni, Determination of effectiveness of transient stability controls using reduced number of trajectory sensitivity computations, IEEE Transactions on Power Systems 19 (2004) 473–482.
[27] J. Ma, D. Han, R.-M. He, Z.-Y. Dong, D.J. Hill, Reducing identified parameters of measurement-based composite load model, IEEE Transactions on Power Systems 23 (2008) 76–83.
[28] I.A. Hiskens, M.A. Pai, Trajectory sensitivity analysis of hybrid systems, IEEE Transactions on Circuits and Systems I: Fundamental Theory and Applications 47 (2000) 204–220.
[29] R.M. Rifaat, On composite load modeling for voltage stability and under voltage load shedding, in: IEEE Power Engineering Society General Meeting, vol. 2, Denver, CO, June 7–10, 2004, pp. 1603–1610.